

The solidification of a magma ocean of Vesta

KAWABATA, Yusuke^{1*}; NAGAHARA, Hiroko¹

¹Earth and Planetary Science, The University of Tokyo

Asteroid 4 Vesta is the only preserved intact example of a large, differentiated protoplanet. Observations of surface spectra of Vesta provide convincing evidence for a differentiated interior. Vesta is considered as the parent body of HED meteorites.

Whether growing mineral grains remain suspended in the magma ocean or settled out is crucial for the primary interior structure of a planet.

The purpose of this study is to understand the role of grain size of crystals on solidification of a magma ocean under a turbulent flow. We select asteroid 4 Vesta as a subject of this study due to the presence of HED chondrites as a reference. In this study, we consider the solidification before the rheological transition occurs.

We assume that the interior structure of Vesta had already differentiated to form a core. We use the bulk silicate Vesta composition proposed by Righter and Drake (1998), which is a mixture of L and CV chondrites with the ratio of 7 to 3 adjusted for core separation. We calculate liquidus, solidus and solid fractions using the MELTs program (Ghiorso and Sack 1995; Asimow and Ghiorso 1998). In vigorously convective systems such as magma oceans, the temperature distribution is nearly adiabatic and isentropic (Solomatov, 2000).

The heat flux can be calculated with the help of the blackbody radiation. This heat flux must match the heat flux transported to the surface by convection. Convection changes to a regime sometimes called hard turbulence at very high Rayleigh number such as those in the magma ocean, of which heat flux is shown by Siggia (1994).

To describe the rate at which particles settle out of a turbulently convective fluid, we use the model by Martin & Nokes (1989). The particle number is calculated by

$$dN/dt = N(-g\Delta\rho a^2)/(18\nu h)$$

where N is the particle number, g is the acceleration due to gravity, a is the diameter of the particle, $\Delta\rho$ is the density difference between the crystal and the magma, ν is the kinematic viscosity, and h is the depth of the fluid layer (Martin & Nokes, 1989).

The adiabat, liquidus and solidus of the magma ocean of Vesta are very steep, that is, they have negligibly small dependence on pressure.

Thermodynamic calculations with the MELTs program showed that olivine is the first liquidus phase at ~1900K, followed by orthopyroxene and spinel. At the very late stage, clinopyroxene appears consuming orthopyroxene if chemical equilibrium is maintained.

The fluid dynamic evaluation shows that a very small fraction of crystals are separated from the magma ocean until the rheological transition which varied from 100 μ m to 1cm in the current work. The thickness increases with time, which is shown in Figure.

Evaluation of fluid dynamic regime shows that the magma ocean on Vesta was at the hard turbulence regime, suggesting near equilibrium crystallization until the rheological transition takes place at the crystal fraction of 60% at 1649K.

The role of grain size on fluid dynamics is very small, but the amount of crystals settled down to the bottom of the magma ocean has small dependence on the grain size. If the crystal size is 1cm, 1km thickness bottom layer is formed.

The fluid dynamic regime changes into soft turbulence in 100 years in the order in the magma ocean of Vesta.

The summary of our conclusion is as follows.

- (1) The pressure effect in the interior of Vesta is negligibly small.
- (2) The solidification of a magma ocean of Vesta before the rheological transition follows batch solidification.
- (3) The size of crystallizing grains has a minor effect on the evolution of magma ocean until the rheological transition.
- (4) The mantle would be harzburgite if the interstitial melt was effectively extracted at the later soft turbulence stage.

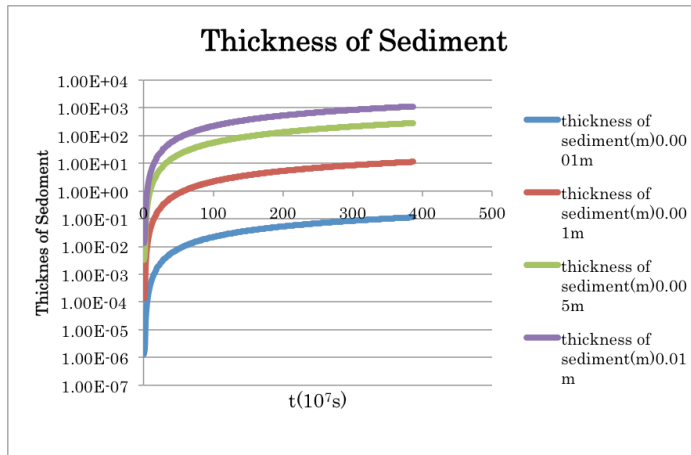
Fig. The thickness of the bottom layer consisting of settled crystals from the main body of a magma ocean.

PPS21-01

Room:416

Time:April 29 09:00-09:15

Keywords: Vesta, magma ocean



Thermal evolution simulation of Vesta including convection and melt migration

NOGAMI, Tatsuhiko^{1*} ; SIRONO, Sin-iti²

¹Division of Earth and Planetary Sciences, Graduate School of Science, Nagoya University, ²Division of Earth and Planetary Sciences, Graduate School of Science, Nagoya University

Vesta has been regarded as the parent body of the HED meteorites. From the observation of DAWN spacecraft, the uppermost layer of Vesta is composed of howardite and its thickness ranges from 50km to 80km (Jutzi et al. 2013). It is known that the ratio of the number of eucrites to diogenites is around two. Based on these facts, rapidly cooled magma layer on Vesta should be more than 10km in thickness.

In this work, I studied the evolution of internal thermal evolution of Vesta due to heating of decay of ²⁶Al. I calculated the temperature distribution by solving numerically heat conduction equation. According to Formisano et al.(2013), if Vesta completed its formation within 1.4Ma from the injections of ²⁶Al into the solar nebula, the degree of silicate melting inside Vesta exceeds 50 vol%. But in that work, convection and melt migration were not taken into account. These two mechanisms contribute to cool down Vesta. It is expected that the formation of Vesta should be completed earlier if these effects are taken into account. On the other hand, it is known that it takes about a few million years for Vesta-size planet to complete its formation according to the standard model of planetary formation.

As a convection model, I adopted the model of Kaula (1979). It was assumed that generated melt migrates to the surface instantaneously, and the migrating melt to the surface was accounted as the rapidly cooled magma. There are two parameters in this study, including a (the percentage of melt migration) and t_0 (formation time of Vesta), and perform simulation taking into account the convection and melt migration.

As a result, convection and melt migration substantially change the evolution of internal thermal structure, and total volume of magma considerably depends on a and t_0 . The magma volume increases as a increases. On the other hand, the magma volume decreases as t_0 increases.

When $t_0=0$, corresponding to no decay of ²⁶Al at the beginning, and if $a>0.3$, the erupting magma layer of 10km in thickness is formed. When $a=1$, corresponding to total melt migration, the magma layer of 10km is formed if $t_0<0.9$ Ma. According to these results, Vesta should be completed its formation within 0.9Ma after CAI formation, and more than 30% of generated melt should migrate the surface. But total generated melt migration is not reasonable. If $a<1$, Vesta has to be formed earlier than $a=1$.

Therefore, it is suggested that the formation time of Vesta should be earlier than the estimate by Formisano et al.(2013), and rapid formation mechanism of 100km sized objects is needed.

Thermal conductivity measurements of sintered glass beads and application to planetesimal thermal evolution

TSUDA, Shoko¹ ; SAKATANI, Naoya^{2*} ; OGAWA, Kazunori³ ; TANAKA, Satoshi³ ; ARAKAWA, Masahiko⁴ ; HONDA, Rie⁵

¹University of Tokyo, ²The Graduate University for Advanced Studies, ³Institute of Space and Astronautical Science, ⁴Kobe University, ⁵Kochi University

In the planetary formation process, dusts in the early solar nebula would have formed into planetesimals. Planets and asteroids have been formed by collisions of planetesimals. To constrain planetesimal's formation process and internal structure is an important issue. Especially, thermal evolution of planetesimal is key phenomenon for this purpose, and thermal conductivity of the planetesimal constituents is an essential parameter for understanding the thermal evolution.

As planetesimals are treated as dust aggregates, they would experience sintering when their temperature increases as a result of thermal evolution. The sintering makes neighbor particles bonded. The thermal conductivity of powdered materials before sintering has been researched recently. However, thermal conductivity of sintered dust has not been measured under vacuum. Once dusts undergo the sintering, contact faces, so-called neck, are formed between dusts. The sintering causes growth of the neck and decrease of the porosity. It is thought that these changes make thermal conductivity higher than not-sintered dusts.

Based on our previous measurements of the thermal conductivity of glass beads, a positive correlation between thermal conductivity and compressional stress (thus, the inter-particle contact area) was observed with sample porosity remaining constant. Therefore, the thermal conductivity should be expressed as a function of not only porosity but also contact area between the particles.

This study aims at investigating thermal conductivity of the sintered materials under vacuum condition, in order to estimate effect of the sintering on thermal evolution of planetesimals. Especially, we focus on the dependence of neck size on the thermal conductivity.

We used three sizes of glass beads (250, 500, and 1000 μm) as analogous samples of dusts. For respective glass beads, we made three sintered samples with different degrees of sintering, or different neck size, in order to investigate the neck size dependence of the thermal conductivity. To measure the neck size, the sintered particles were separated and the neck crack size was observed using optical microscope. The thermal conductivity was measured by line heat source method under vacuum.

As a result of these experiments, we confirmed that the neck sizes of the nine samples had different ratio of neck size to beads radius, whose average values were ranged from 0.075 to 0.30. The thermal conductivity was ranged from 0.036 to 0.25 W/mK. These values were more than 10 times higher than that of not-sintered glass beads. Combining the results of neck size and thermal conductivity measurements, it was found that the thermal conductivity is proportionally related to the neck size ratio independent of the particle size. In these experiments, the porosity was constant about 40%. Therefore, when we calculate thermal evolution of planetesimals under sintering, the thermal conductivity should be estimated from the neck size at least until the neck size ratio grows up to 0.3 (initial stage of sintering).

Finally, we calculated the thermal evolution of the planetesimal using the relation of the thermal conductivity and the neck ratio we found in this experiment. Hypothesized planetesimals have radius between 100 m and 1000 m, formation age between 1 Myr and 3 Myr after CAI formation, and dust diameter of 1 and 1000 μm . As a result of the calculation, it was found that the sintering and resulting increase of the thermal conductivity make internal peak temperature more than 1000 K lower than the case when the sintering effect is not included in the calculation. In addition, internal temperature structure and neck size (or material strength) distribution in the planetesimals vary widely depending on the size and formation age of the planetesimals and particle size of dust.

The effect of melt on frictional behavior and the implication for deep moonquake

AZUMA, Shintaro^{1*} ; KATAYAMA, Ikuo¹

¹Department of Earth and Planetary Systems Science, Hiroshima University

Apollo program (Passive Seismic Experiment) investigated a number of seismic events in moon (e.g., Nakamura 2003). These seismic events (moonquakes) are classified to four categories; thermal moonquake, shallow moonquake, impact moonquake and deep moonquake (Latham et al., 1969). In kinds of moonquake, deep moonquake is especially interesting because the occurrence depth of deep moonquake (700~1200 km) is obviously in plastic deformation region where frictional behavior and fracture does not occur. Analysis of PSE (Passive Seismic Experiment) data and modelling in previous studies suggest that the partial melt layer underlies near the occurrence depth of deep moonquake (Weber et al., 2011). Therefore partial melt possibly is one of important factor on the deep moonquake. Here we show the results of frictional experiments using a boronated diphenylamine which can be adjusted in melt fraction and dihedral angle (Takei 2000). When dihedral angle is 30°, frictional coefficient becomes small with decrease of melt fraction. Although frictional coefficient is significantly decreased when dihedral angle is 0°, frictional coefficient does not depend on melt fraction. When dihedral angle of partial melt is 0°, frictional behavior is fully dominated by partial melt. Partial melt is considered to have the three effects on the shear strength. First, our frictional experiments found that partial melt decrease frictional coefficient. Second, partial melt behave as the pore pressure. Third, partial melt extracts the water from the surrounded rocks, and induces the shear localization (the stress concentration). Considering these effects of partial melt on frictional behavior, partial melt might be one of important factors on deep moonquake.

Keywords: melt, deep moonquake, moon, frictional behavior

Velocity scaling of granular convection and its application to timescale of regolith migration

YAMADA, Tomoya^{1*} ; KATSURAGI, Hiroaki¹

¹Graduate School of Environmental Studies, Nagoya University

On the basis of accurate surface observation of asteroid Itokawa, it has been thought that regolith migration and sorting could occur [1]. Besides, Nagao et al. revealed that cosmic-ray exposure age of Itokawa's surface grains is less than 8 Myr [2]. As a possible explanation for such active and young surface of Itokawa, regolith convection caused by impact-induced seismic shaking has been considered [1]. Indeed, granular convection can be readily observed in the laboratory experiment of vertically vibrated granular matter (e.g. [3]). However, the quantitative feasibility of granular convection under the microgravity environment has not been studied well so far. Although the direct control of gravity is quite difficult, we instead employ the scaling approach to figure out the gravity dependence of granular convective velocity. Specifically, we measure the granular convective velocity under various experimental conditions. Then, using the systematically obtained data, we find a scaling relation among the convective velocity, gravitational acceleration, and other control parameters such as vibration frequency, grain size, and so on. We also estimate the timescale of regolith migration due to the granular convection by using the obtained scaling.

The grains used in this experiment are glass beads of diameter $d = 0.4, 0.8, \text{ or } 2 \text{ mm}$ (AS-ONE corp. BZ04, BZ08, BZ2). The experimental setup consists of a cylinder made by plexiglass of its height 150 mm and inner radius $R = 16.5, 37.5, \text{ or } 75 \text{ mm}$. The cylindrical cell is filled by glass beads to make a granular bed of the height $H = 20, 50, 80, \text{ or } 110 \text{ mm}$. The system is mounted on an electromechanical vibrator (EMIC 513-B/A) and shaken vertically. The vibration frequency f is varied from 100 to 300 Hz and the maximum dimensionless acceleration is varied from 2 to 6 . Motions of glass beads on the sidewall of the container are captured by a high-speed camera (Photoron SA-5) with a macro lens. PIV (Particle imaging velocimetry) method is used to compute the vertical component of the convective velocity, v_z . The maximum value of the velocity is nondimensionalized as $v_{zmax}/(gd)^{1/2}$, where g is the gravitational acceleration. Using the obtained experimental data, we scale $v_{zmax}/(gd)^{1/2}$ by the shaking parameter S [4] and the dimensionless system size L . S represents the energy balance between vibration and gravity, $S=(2\pi Af)^2/gd$, where A is shaking amplitude. L is the scaled system size defined by $L=(RH)^{1/2}/d$.

As a result of systematic dimensional analysis, we obtain a scaling form, $v_{zmax}/(gd)^{1/2} \sim S^{0.47}L^{0.82}$. From this scaling form, we find that the granular convective velocity v_{zmax} depends on the gravitational acceleration g as $v_{zmax} \propto g^{0.97}$ when the maximum dimensionless acceleration is fixed. This means that the granular convective velocity is almost proportional to the gravitational acceleration. We also find that the timescale of regolith migration due to the granular convection is almost independent of its roll size, by assuming that L is the dimensionless convective roll size. In the presentation, we are going to discuss the consistency between the regolith migration timescale and cosmic-ray exposure age of Itokawa's surface grains.

[1]H. Miyamoto *et al.*, Science **316**, 1011 (2007)

[2]K. Nagao *et al.*, Science **333**, 1128-1131 (2011)

[3]A. Garcimartín *et al.*, Physical Review E **65**, 031303 (2002).

[4]P. Eshuis *et al.*, Physics of Fluids **19**, 123301-1 (2007)

Keywords: granular convection, scaling analysis, gravitational acceleration, regolith migration, Itokawa

Experimental study on impact-induced seismic wave propagating in granular materials

MATSUMOTO, Eri¹ ; YASUI, Minami^{2*} ; ARAKAWA, Masahiko¹

¹Graduate school of Science, Kobe University, ²Organization of Advanced Science and Technology, Kobe University

Introduction:

A seismic wave survey is a direct method to investigate the sub-surface structures of solid bodies, so we measured and analyzed these seismic waves propagated through these interiors. Earthquake and Moonquake are the only two phenomena that have been observed to explore these interiors until now, while the future surveys on the other bodies, (solid planets and/or asteroids) are now planned. To complete the seismic wave survey during the mission period, the artificial method that activates the seismic wave is necessary and the one candidate for the artificial one is a projectile collision on the target body. However, to utilize the artificial seismic wave generated on the target body, the relationship between the impact energy and the amplitude and the decay process of the seismic wave should be examined. If these relationships are clarified, we can estimate the required sensitivity of seismometers installed on the target body and the distance from the seismic origin measurable for the seismometer. Furthermore, if we can estimate the impact energy from the observed seismic wave, it is expected to estimate the impact flux of impactors collided on the target body. In this study, we carried out impact experiments in the laboratory, observed the seismic waves by accelerometers, and examined the effects of projectile properties on the amplitude and the decay process of the seismic wave.

Experimental methods:

We did impact experiments by using the one-stage gas gun at Kobe University. The projectile was a polycarbonate cylinder with the diameter of 10 mm and the height of 10 mm, and a stainless and an alumina ball with the diameter of 3 mm. The stainless and the alumina balls were accelerated with the sabot made by polyethylene. The impact velocity was ~ 100 m/s. The target was prepared by putting 200 μm glass beads into the container with the diameter of 300 mm and the height of 100 mm, up to 80 mm depth. Three accelerometers (response frequency < 10 kHz) were set on the target surface at different distances from the impact point. The observed seismic waves were recorded as voltage on the data logger (A/D conversion efficiency 100 kHz).

Experimental results:

We calculated the propagation velocity of seismic wave by using the traveling time from the impact point to the site of accelerometer and the impact velocity, and obtained 105 ± 15 m/s. Additionally, the relationship between the maximum acceleration, g_{max} , and the normalized distance, x/R (x : distance from impact point, R : crater radius), was determined as $g_{max} = 268(x/R)^{-2.8}$. From these results, it is found that the seismic wave attenuates with similar waveform on the same target, irrespective of projectile type. The duration keeping the maximum acceleration was estimated to be ~ 0.3 ms, and this value was almost consistent with the penetration time of projectile estimated by using the model proposed by Niimi *et al.* (2011). McGarr *et al.* (1969) studied the energy conversion efficiency from impact energy to seismic momentum and obtained the ratio of the impulse of projectile during the penetration, I , to the kinetic energy of projectile, E_k . As a result of this study, the I/E_k was obtained to be $1.6 \times 10^{-2} \pm 1.0 \times 10^{-2}$. On the other hand, McGarr *et al.* (1969), which the lexan projectile collided on the sand target with the impact velocity of 2-8 km/s, was obtained to be $6 \times 10^{-6} \pm 4 \times 10^{-6}$. This difference might be caused by the dependence of impact velocity on the energy conversion efficiency.

Keywords: impact-induced seismic wave, granular materials, decay process, planetary exploration, crater formation, accelerator

Velocity measurements of impact jetting during oblique impacts

KUROSAWA, Kosuke^{1*}; NAGAOKA, Yoichi¹; HASEGAWA, Sunao²; SUGITA, Seiji³; MATSUI, Takafumi¹

¹PERC, Chitech, ²ISAS, JAXA, ³Dept. of Complexity Sci. & Eng., The Univ. of Tokyo

Impact jetting is a widely-known phenomenon in both hypervelocity impact experiments and hydrocode calculations. There are two important features in impact jetting, which are (1) extremely high velocity greater than the impact velocity and (2) the high degree of shock heating. Jetting has been considered as a mechanism for the origin of chondrules, tektites and impact glasses, Pluto, and the Moon. Jetting during a symmetric collision between two thin plates has been well studied. However, the understanding of jetting for spherical impactors is essential for planetary applications and it has not been obtained. One of the reasons for this is the lack of the experimental data of hypervelocity jetting of obliquely-impacted spherical projectiles. Although the temperature of jetted vapor has been investigated under a wide range of experimental conditions, only 3 data points, including unpublished data, have been reported as the jet velocity, which is one of the important anchors for developing a jetting model.

In this study, we conducted a series of oblique impact experiments using spherical projectiles and 3 different targets and investigated the jet velocity as a function of impact velocity and target materials. The frame rate of a high-speed imaging was 100 ns/frame to resolve the jetting initiation during projectile penetration. We found that the velocity ratio of the jet velocity to the impact velocity increases as the shock impedance of target increases at a given impact velocity and decreases with as impact velocity increases.

We obtained the first systematic data set for the jet velocity of spherical projectiles during oblique impacts. Using the data set, we constructed a physical model to explain the observed jet velocities. We found that (1) a classical phenomenological model constructed by Ang (1990) predicts well observed jet velocities if we use the vertical component of impact velocity instead of impact velocity in his model and that (2) observed jet velocities can be obtained by the sum of the horizontal component, the deformation velocity of the shocked projectile, and the particle velocity after isentropic release. The latter model may provide a physical basis of the jet formation

Both the standard and our physical model predict the jet velocity during oblique impacts reaches 2.5 times than the impact velocity. Although the mass of jetted materials must be small for energy conservation, the aerodynamic interaction between such hypervelocity jet and an ambient atmosphere may be significant because the heating rate of aerodynamic ablation is proportional to the cube of the velocity. In the case for an oblique impact on Titan, the jet velocity may reach 30 km/s in the case of typical cometary impacts and may generate strong EUV radiation from produced high-temperature plasma in the N₂CH₄ atmosphere via aerodynamic interaction near the surface of Titan. Active chemical reactions of C-bearing species may be driven by the produced EUV. The available energy source near the current Titan surface is only cosmic rays. Thus, hypervelocity jetting may be a new energy source for atmospheric chemistry on Titan.

Keywords: Hypervelocity impacts, Oblique impacts, High-speed video camera, Ultrafast imaging observation, Impact jetting, Titan

The stability of amino acids in early ocean by meteorite impacts: Implication for chemical evolution of biomolecules

UMEDA, Yuhei^{1*} ; SEKINE, Toshimori¹ ; FURUKAWA, Yoshihiro² ; KAKEGAWA, Takeshi² ; KOBAYASHI, Takamichi³

¹Graduate School of Science, Hiroshima University, ²Graduate School of Science, Tohoku University, ³National Institute for Materials Science

Prebiotic oceans may have contained abundant amino acids, and were subject to meteorite impacts, especially during the late heavy bombardment. It has been unknown how meteorite impacts affected such dissolved amino acids in the early oceans. Experiments in the present study were performed using aqueous solutions containing olivine or hematite powders and ¹³C-labeled glycine and alanine. In particular, the reaction products from ¹³C-labeled amino acids are expected to compose ¹³C, distinguishing if they are contaminants or not. Two powders of olivine and hematite help to keep the oxygen fugacity low and high during experiments, respectively in order to investigate the effect of oxygen fugacity on chemical reaction of amino acids. The run product of selected amino acids and amines in samples were analyzed with liquid chromatography-mass spectrometry (LC/MS). Some experiments were carried out in the presence of ammonia and/or benzene. The results revealed that amino acids survived partially or reacted out in early ocean through meteorite impacts. It was found that glycine changes into alanine and large amounts of methylamine and ethylamine are formed. Amine formation from alanine was increased considerably in the presence of Fe₂O₃ rather than olivine under similar impact conditions. XRD for the recovered hematite powders indicated the presence of a small amount of magnetite, suggesting that the oxygen fugacity was kept high enough to be close to the Fe₂O₃-Fe₃O₄ buffer. The formation of n-butylamine, detected as the largest number of carbon species in the recovered samples from the solutions with ammonia and benzene, suggests that chemical reactions to form new biomolecules can proceed through marine impacts. These results suggest that amino acids in early oceans can proceed further by impact-induced reactions, implying that impact energy plays a role in the prebiotic formation of various biomolecules, although the reactions depend upon the chemical environments as well.

Organic aerosol experiments for CH₄/CO₂ atmospheres using a hydrogen/helium UV lamp

HONG, Peng^{1*} ; SEKINE, Yasuhito¹ ; SUGITA, Seiji¹

¹Complexity Sci. & Eng., Univ. of Tokyo

Organic aerosols are photochemically produced in CH₄-rich reducing atmospheres, but their production mechanisms are not well constrained. Organic aerosol layers are believed to influence the surface temperature of early Earth, through its anti-greenhouse (Pavlov et al., 2001) and/or indirect greenhouse effects (Wolf and Toon, 2010), however, because of the uncertainty of the aerosol production mechanism, there are large uncertainties inherent in previous estimates of the aerosol production rate and optical depth of aerosol layers (Trainer et al., 2006). In order to put a constraint to the production mechanism and obtain aerosol production rate applicable to CH₄/CO₂ atmospheres, we conducted laboratory experiments to form organic aerosol analogues using a hydrogen/helium lamp that simulates solar far UV (FUV) with wavelengths longer than 110 nm. We measured the aerosol production rate as functions of UV flux and of CH₄/CO₂ ratio in the reactant gas. The aerosol production rates were determined by ellipsometrically measuring the growth rates of thin organic films deposited on a substrate. The UV fluxes from the hydrogen/helium lamp were measured by N₂O/CO₂ actinometry. Our experimental results show that the aerosol production rate is not a second-order function but a linear function of UV flux. This leads to a lower estimate for aerosol production rate due to FUV irradiation, when extrapolating the production rate in Titan's atmosphere to early Earth and exoplanets. We also found that the aerosol production exhibits a steep decrease when the CH₄/CO₂ ratio becomes less than unity. In order to interpret the dependence of aerosol production rate on the CH₄/CO₂ ratio, we also performed one-box photochemical calculations, including 791 reactions and 134 species up to C₈ hydrocarbons. The one-box photochemical model was validated against some basic carbon species (CH₄, C₂H₂, C₂H₄, C₂H₆, CO, CO₂), in which the abundances of those species calculated with the model and observed with a quadrupole mass spectrometer (QMS) show a good agreement. We found that the observed production rate is in a good agreement with polymerization reaction rates involving aromatic hydrocarbons (i.e., benzene), suggesting benzene is the key parent molecule controlling the aerosol production. On the other hand, polymerization reactions involving polyynes do not account for the experimental data, suggesting that they are not the limiting molecules. This implies that aerosol production rate in an early Earth atmosphere due to solar FUV would become significantly lower than a previous estimate which includes polymerizations of polyynes as formation reactions of aerosols (Pavlov et al., 2001), resulting in an optically thinner aerosol layer by a factor of 100. Thus the optical depth of organic aerosol layers produced by solar FUV in an early Earth atmosphere would not have had efficient anti-greenhouse effect or indirect greenhouse effect, which makes other greenhouse effect important for the Archean climate, such as greenhouse effect of ethane. We will also discuss the possibility of aerosol formation through nitrile reactions driven by high-energy particle irradiation, which could be more efficient than the aerosol production due to solar FUV.

Keywords: organic aerosol, photochemistry, laboratory experiment, reducing atmosphere

Proto-atmosphere on giant icy satellites forming within gaseous circum-planetary disks

MIKAMI, Takashi^{1*} ; KURAMOTO, Kiyoshi¹

¹Department of CosmoSciences, Graduate School of Science, Hokkaido University

In spite of the great similarity in size and mean density, the giant icy satellites Ganymede, Callisto, and Titan have very different surface environments. In particular, only Titan holds a thick atmosphere dominated by N₂. Recent data of the Cassini spacecraft indicated that atmospheric N₂ is probably originated from other nitrogen-bearing species like NH₃. However, it still remains an open question when and how N₂ was generated. This is partly because the physical states of giant icy satellites have been poorly understood.

According to a widely-accepted theory of regular satellites formation, the giant icy satellites were formed in subnebulae with low temperature and low pressure taking a long accretion time. Some models assert that their surfaces were kept too cold to induce significant differentiation during accretion. However, these satellites may capture a significant amount of subnebula gas, which possibly forms proto-atmospheres along with gases volatilized from icy components. Such a hybrid-type proto-atmosphere may have significant blanketing effect.

Here, we numerically analyze the structure and effect of a hybrid-type proto-atmosphere. Our model atmosphere is hydrostatically connected with subnebula at the satellite Hill radius. It contains H₂ and He as nebula gas components, H₂O and NH₃ as volatilized ice components. The radiative-convective equilibrium structure is solved as a function of surface temperature. The subnebula conditions are given by Canup and Ward (2002), the temperatures are 150 K at Ganymede, 120 K at Callisto, and 50 K at Titan, and the corresponding subnebula pressures are varied over 0.1-10 Pa.

For all the boundary conditions, the proto-atmosphere is opaque due to water vapor, so that the outgoing thermal radiation (OTR) flux at top of the atmosphere is smaller than that of black body radiation without atmosphere when the surface temperature is higher than 273 K. When the surface temperature is lower, the OTR fluxes from the proto-atmospheres of Ganymede and Callisto are close to black-body radiation because these atmospheres have low surface pressure and are optically thin due to large scale height under high background temperature. On the other hand, the proto-atmosphere of Titan has another type of solution with the OTR fluxes significant lower than blackbody radiation under low surface temperature. This is due to the formation of optically thick atmosphere tightly bounded by gravity because of low background temperature.

These results imply that a warm proto-atmosphere near 200 K could be kept on Titan for a long time after the end of accretion. Our stability analysis suggests that the proto-atmospheres of Ganymede and Callisto were lost associated with the dissipation of the Jovian subnebula, but that of Titan survived after the dissipation of the Saturnian subnebula.

In the case, NH₃ vapor pressure would be kept high under the irradiation of the solar UV for a long time. The present atmospheric N₂ of Titan may be generated by photochemical reaction of NH₃ vapor in such a warm proto-atmosphere.

Keywords: Giant icy satellite, Atmosphere, Circum-planetary disk

Atmospheric formation and thermal evolution of a proto-Mars growing in the solar nebula

SAITO, Hiroaki^{1*} ; KURAMOTO, Kiyoshi¹

¹Cosmo Sci., Hokkaido Univ

It is widely accepted that Mars is a survivor of proto-planets formed by oligarchic growth i.e., the runaway accretion of planetesimals. Numerous planetesimals impacts onto the growing proto-Mars likely cause shock-melting, resulting into the early core formation as constrained by the chronology of Martian meteorites. Such impacts should also induce the degassing of H₂O and other molecular species from accreting materials, which contributes to atmosphere formation. Since the oligarchic growth proceeds within the solar nebula, a growing Mars probably acquired a proto-atmosphere consisting of the mixture of nebula gas component and degassed component. Such a hybrid-type proto-atmosphere may play important role in thermal balance and volatile partitioning between the planetary surface and interior. However, the structure and behavior of such atmosphere has been poorly investigated so far.

In this study, we build a one-dimensional radiative-convective (RT) equilibrium model for a hybrid-type proto-atmosphere assuming a compositional double layer structure. Here the upper layer is dominated by H₂-He continuing from the solar nebula and the lower one is dominated by degassed components enriched in H₂O. Radiative transfer is modeled, taking into account the absorptions by H₂, He and H₂O. RT equilibrium structures are obtained as a function of thermal luminosity that would be balanced with accretional heating rate and the amount of degassed component. The degassed component consists of H₂O and H₂ with molar ratio 1:5 in equilibrium with metal and silicate. The accretion time is taken 10⁶-10⁷ years.

For the pure H₂-He atmosphere, the surface temperature is kept lower than 700 K. Supply of degassed component increases the surface temperature that can exceed 1500 K given the mass of degassed component more than 1% of the Mars mass. If planetesimals contain enough proportions of H₂O and other heavy volatiles, growing Mars would have global magma ocean sustained by the blanketing effect of proto-atmosphere. This would promote core formation and transport of dissolved volatiles.

Line-by-line calculations of radiation properties for exoplanets with steam atmosphere

ONISHI, Masanori^{1*} ; HASHIMOTO, George² ; KURAMOTO, Kiyoshi³ ; TAKAHASHI, Yoshiyuki O.¹ ; TAKAHASHI, Yasuto³ ; ISHIWATARI, Masaki³ ; HAYASHI, Yoshi-yuki¹

¹Department of Earth and Planetary Sciences, Kobe University, ²Department of Earth Sciences, Okayama University, ³Department of Cosmochemistry, Graduate School of Science, Hokkaido University

For a hot water rich atmosphere, there is an upper limit on the thermal emission that is unrelated to surface temperature (Simpson, 1927, Nakajima et al., 1992). The radiation limit is deeply related to evolution of planetary atmosphere. Hamano et al., 2013 showed that terrestrial planets can be divided into two distinct types on the basis of their evolutionary history during solidification from the initially hot molten state depending on whether incoming flux from a host star is larger or less than the radiation limit. On the other hand, the first direct image of an exoplanet has finally occurred in 2004 (Chauvin et al., 2004), it is expected to observe radiation spectrum from terrestrial planets near future. If we can observe the spectrum, we have potential to clarify the atmospheric and surface environment and history of the planets. In order to estimate the planetary environment from the observation, numerical simulation of radiative transfer is needed. The most reliable calculation method of the radiation is line-by-line treatment. Goldblatt et al., 2013 calculates the radiative transfer of a pure water atmosphere by line-by-line treatment. Goldblatt et al., 2013 investigates only one case of surface water amount, one current ocean mass case. In this study, we calculate the radiative transfer in steam atmosphere by line-by-line treatment in several surface water amount cases.

Absorption cross section of water vapor was calculated from HITRAN2010 (Rothman et al., 2010) and MT_CKD continuum model (Mlawer et al., 2012). We used a 1D convective model in pure water atmosphere. The surface temperature was varied from 250 to 2000 K. The total water amount of water was varied from 0.01 to 5 current Earth ocean mass (270 bar). For rapid calculation, we prepared absorption cross section table and calculated required absorption cross section by cubic spline interpolation. A two-stream approximation (Toon et al., 1989) was used to calculate radiative transfer by line-by-line treatment with resolution of 0.01 cm^{-1} wavelength.

A radiation limit of our study is 282 W m^{-2} . The value is in good agreement with that of Goldblatt et al., 2013. When the total water amount is lesser, increasing of outgoing thermal flux over radiation limit occurs in lower surface temperature conditions. In 0.01 current ocean mass condition, increasing of flux occurs in lower than 1000 K. In this case, most of flux radiate from 10 micron and 4 micron window region. Results of optical depth calculation indicate that we can't detect NIR and IR radiation from the surface of planets with surface temperature higher than 1500 K, even if the planet has 0.01 water amount.

Keywords: steam atmosphere, radiative property, radiation limit

Dependence of the runaway threshold on water distributions on the surface of Earth-like planets

NITTA, Akira^{1*} ; ABE, Yutaka¹ ; O'ISHI, Ryouta² ; ABE-OUCHI, Ayako²

¹Department of Earth and Planetary Science, Graduate School of Science, University of Tokyo, ²Atmosphere and Ocean Research Institute, University of Tokyo

Liquid water is one of the most important material not only for its large effect on planetary climate but also as a controlling factor of the habitability [e.g. Kasting et al., 1993]. Water planets, which are planets with liquid water on their surface, can be divided in 3 types: 'ocean planets', 'partial-ocean planets', and 'land planets'. Ocean planets have enough water to cover their surface entirely. Partial-ocean planets, which are like the Earth, have an interconnected ocean and lands. Land planets have little water in scattered lakes around both Poles [Abe et al., 2013, Hawaii, Kona]. The type of the water planet is determined by the balance between the surface water transport, which depends on the amount of water and topography, and the atmospheric water transport, which depends on the global circulation.

Surface water on each water planet is unstable and entirely vaporized when the planet receives insolation above a certain critical value. It is because of the positive feedback of the greenhouse effect of water vapor. This phenomenon is called the runaway greenhouse. In the following, the critical insolation is called 'runaway threshold' [e.g. Abe and Kasting 1988; Nakajima et al, 1992; Kopparapu et al., 2011].

Abe et al. [2011] discussed the difference of the runaway threshold between Earth-sized ocean planets and land planets using a 3-D model for the first time. They found that the surface water of land planet is significantly stable than that of ocean planet against the large insolation. While an ocean planet gets unstable and the runaway greenhouse occurs when the insolation reaches about 130% of that on the present Earth, a land planet remains stable until the insolation reaches 170%. However, a land planet that they represented is only one of the various situations of land planets, and they didn't mention the effect of variety of surface water distributions on the planetary climate.

Takao [2013] showed the dependence of the runaway threshold on latitudinal surface water distribution using the combination of meridional energy balance model (EBM) and the vertical radiative-convective equilibrium model. He suggested that runaway threshold of the Earth-sized water planet varies with the degree of latitudinal localization of surface water. Nevertheless, his 1-D EBM was so simple that he could neither discuss about the effects of longitudinal distribution of surface water, nor include dynamical global circulation.

In this study, we perform numerical experiments to clarify the effects of the surface water distribution on runaway threshold of Earth-sized planets with a 3-D model, GCM.

We use CCSR/NIES AGCM 5.4g [Numaguchi, 1999], which includes dynamical atmospheric circulation, radiative transfer, formation of clouds, and so on. While this model is adapted to the present Earth, it cannot calculate the change of surface water distribution determined by the water amount and topography. Therefore, we assumed the surface water distribution, which is determined as a result of the balance between the surface and atmospheric water transport in reality, and used it as the boundary condition. Then, we raised the insolation gradually until the surface water got unstable for each surface distribution, and evaluated the runaway threshold.

We found that the degree of localization of surface water significantly affects the runaway threshold, and it varies from 180% (extremely localized land planet) to 130% (ocean planet) continuously. Even if no surface water is given low latitudes area initially, because the Hadley circulation transports water to such area, when the initial surface water area reaches adequately low latitudes, the runaway threshold is almost the same as that of ocean planets, that is, 130%. We also investigated the dependence on the longitudinal water distribution. As a result, even if the total area of surface water is the same, there are about 10% of differences in the runaway threshold depending on its distribution.

Keywords: runaway greenhouse, GCM, Earth-like planet

Dead zones by electric heating in protoplanetary disks

MORI, Shoji^{1*} ; OKUZUMI, Satoshi¹

¹Tokyo Institute of Technology

Turbulence driven by magnetorotational instability (MRI) is a viable mechanism of angular momentum transport in accretion disks. In protoplanetary disks, however, there is a region where the ionization degree is too low for MRI to be active (e.g., Gammie 1996; Sano et al. 2000). Whether turbulence is present or not strongly affects the growth of dust particles to planetesimals. Therefore, a good knowledge of the size of dead zones is essential to understanding planet formation.

In this study, we focus on the heating of electrons by turbulent electric fields and its effect on the ionization state of protoplanetary disks. Previous studies have assumed that electrons in the disks have the same temperature as the neutral gas. However, this is not necessarily the case in MRI-driven turbulence, in which turbulent electric fields can significantly heat up electrons (Inutsuka & Sano 2005). Heated electrons efficiently adsorb onto dust grains, and therefore electron heating leads to a reduction of the ionization degree (Okuzumi & Inutsuka, in prep.). This could effectively increase the dead zone size by reducing the saturation level of MRI turbulence outside the conventional dead zone.

The aim of this study is to show where in protoplanetary disks the effect mentioned above becomes important. We calculate the ionization degree of disks assuming that MRI operates outside the dead zone. For a minimum-mass solar nebula with the dust grain radius of 0.1 μm and dust-to-gas mass ratio of 0.01, we find that the effect becomes significant in a region extending from the outer edge of the dead zone (at ~ 20 AU from the central star) out to 70 AU. Furthermore, our analytic estimate suggests that the saturation level of turbulence in this region is significantly low.

Keywords: protoplanetary disk, ionization degree, dust grains, MHD turbulence, electric heating

Collisional disruption of sintered dust aggregates

SIRONO, Sin-iti^{1*} ; UENO, Haruta¹

¹Graduate School of Environmental Sciences, Nagoya University

Planets are formed in a protoplanetary nebula consisting of gas and dust grains. The first step of planetary formation is coagulation of dust grains, leading to the formation of dust aggregates. Further growth of the dust aggregates is promoted by mutual collisions between them. The motion of dust aggregates gradually decouples from that of the gas as aggregates grow. Dust aggregates drift inward due to gas drag. If the inward drift is faster than aggregate growth, solid components in a protoplanetary nebula disappears and planets cannot be formed. To prevent infalling, many mechanisms have been proposed (Kretke & Lin 2007, Lyla et al.2009, Sandor et al.2011). Fast collisional growth during the infalling of icy dust aggregates (Okuzumi et al. 2012) is another possibility. These studies are based on the assumption that the motion of aggregates decouples from gas. The infalling velocity is on the order of 1m/s when substantial decoupling is attained. Aggregates should grow to the sizes corresponding to the infalling velocity. Is it possible?

Experimentally, collisional breakup velocity of micron-sized SiO₂ dust aggregates is on the order of 1m/s(Blum 2010). Breakup velocity for H₂O ice aggregates is also on the same order(Shimaki & Arakawa 2012). However, it is difficult to produce highly porous dust aggregates experimentally due to the Earth's gravity. I conducted two-dimensional numerical simulation of sintered dust aggregates in this study. It has been pointed out that sintering of H₂O ice proceeds in wide region of a protoplanetary nebula (Sirono 2013). As sintering proceeds, a neck between adjacent grains grows and mechanical interactions between grains greatly change. The effects of sintering are taken into account by changing breaking forces of a contact. The interactions between non-sintered contacts (Dominik & Tielens 1997) are adopted for newly formed contacts.

If sintering proceeds sufficiently such that a neck is disappeared, catastrophic disruption was observed at low collision velocities (~10cm/s). This is because a contact is broken by rolling of a grain. On the other hand, catastrophic disruption at low collision velocities was not realized for less-sintered aggregates. This is due to immediate reconnection between grains with a non-sintered mode. These results depends on the tensile strength of H₂O ice. The breakup velocity increases as the strength increases. From the results obtained in this study, the evolution of icy dust aggregates is various, depending on the location in a protoplanetary nebula.

Keywords: dust aggregate, protoplanetary nebula, collisional disruption, sintering

Planetesimal size and protoplanetary disk turbulence

KOBAYASHI, Hiroshi^{1*} ; TANAKA, Hidekazu² ; OKUZUMI, Satoshi³

¹Nagoya University, ²Institute of Low Temperature Science, Hokkaido University, ³Tokyo Institute of Technology

When the random velocities of bodies are greater than their surface escape velocities, the runaway growth of bodies occurs, which produces a single large bodies surrounded by leftover bodies in each annual of a protoplanetary disk. The slope of the size distribution of bodies becomes steeper through runaway growth. The slope of runaway growth is seen in the size distribution of 100km sized or larger bodies in the main belt. Since the random velocities rises by turbulent stirring in the disk, the planetesimal size above which runaway growth occurs is determined by the strength of turbulence. We discuss turbulence strength in the solar nebula.

Keywords: Planetesimal, Protoplanetary disk, Asteroids, The size distribution of bodies, Planet formation

The formation of gas planets from cores in type I migration

MAESHIMA, Naohiko^{1*} ; WATANABE, Sei-ichiro¹

¹Division of Earth and Planetary Sciences, Graduate School of Science, Nagoya University

Many gas planets have been discovered. The formation of the gas planets requires that solid planets, which correspond to cores of gas planets, must achieve the critical core mass M_{crit} before the disk gas have entirely diffused. The cores moves radially by torques caused by interaction with disk gas (type I migration). It was long thought that the cores fall into the star with very short timescale before achieving M_{crit} by strong negative torque (Ward 1997, Tanaka et al. 2002). Recent study have showed that the region where positive torque operates is formed on the disk by corotation torque if we consider the non-isothermal process of the gas (Baruteau & Masset 2008,Paardekooper & Papaloizou 2008). As a result, equilibrium radii, where torque is zero, are created. The cores may accrete gas without falling into the star if they are trapped by equilibrium radius because the timescale of radial migration slows down to that of disk evolution. However, positive torque only operates for cores in limited mass range ($M_{p,min} < M_p < M_{p,max}$). If it takes long time for achieving $M_{p,min}$, the cores moves inward largely by negative torque. In this study, we examine how the orbit and mass of cores evolve depending on the disk model, and find the condition the disk must have for the gas planet formation.

The distribution of the gas surface density evolves by viscous diffusion and photoevaporation. The temperature distribution is determined by viscous heating and stellar irradiation. In the disk, an equilibrium radius is formed on the region where the main heating source shifts from the viscous heating to stellar irradiation. In this study, we investigate the possibility of the formation of gas planets at the equilibrium radius. Cores grow by accreting planetesimals in their gravitational radius, and capture the disk gas if they achieve M_{crit} .

We find that the condition of gas planet formation is determined as follows. In disks evolving fast (α parameter of viscosity = 0.005), cores born in the middle region (~ 10 AU) is captured by the equilibrium radius and capture the disk gas by achieving M_{crit} if core growth stars at the time when disk mass is still large (initial mass accretion rate $\sim 10^{-7} M_{\odot} yr^{-1}$) and the ingredient of the cores is abundant (ratio of the solid material to gas is large >0.03). On the other hand, in the disks evolving slowly ($\alpha = 0.001$), gas planets can be formed even if core growth stars at the stage when disk mass has been decreased (initial mass accretion rate $\sim 10^{-8} M_{\odot} yr^{-1}$). In this case, the dependence on the ratio of the solid to gas is very weak.

Keywords: type I migration

Protoplanet Spin by Planetesimal Accretion

SHIBATA, Takashi^{1*}; KOKUBO, Eiichiro²

¹University of Tokyo, ²National Astronomical Observatory of Japan

In the standard scenario of planet formation, protoplanets or planetary embryos are formed through runaway and oligarchic growth of planetesimals. We investigate the spin parameters of protoplanets using N-body simulations. By N-body simulations we can calculate consistently the orbital, accretionary, and spin evolution of planetesimals. The spin of protoplanets are important for terrestrial planet formation since it affects the accretion condition of protoplanets and determines the spin of terrestrial planets. For the standard model of a planetesimal disk, a Mars-sized protoplanet forms in 0.5 million years around 1 AU. We find that the spin angular velocity of planetesimals decreases as their mass increases. Planetesimals obtain their spin angular momentum on the early stage of accretion where their mass ratio is not so large. Once a runaway-growing planetesimal (protoplanet) becomes large enough, it mainly accretes smaller planetesimals whose collisional angular momentum tends to cancel out since they collide from random directions. Thus the protoplanet increases its mass but not the spin angular momentum, which leads to smaller angular velocity for larger protoplanets. When a protoplanet reaches the isolation mass, its typical spin angular velocity is as high as 10% of the critical angular velocity for rotational instability under the assumption of perfect accretion in collisions. We find that the obliquity of planetesimals is well expressed by an isotropic distribution. During the protoplanet growth, the scale height of the planetesimal system is much larger than the size of planetesimals. Thus, collisions are three-dimensional and isotropic, which leads to the isotropic obliquity distribution. We show the dependence of the spin parameters on the initial planetesimal system parameters. The spin angular velocity increases with the bulk density of planetesimals. The dependence of the spin angular velocity on the planetesimal mass becomes weaker as the initial mass of planetesimals increases. However, these system parameters do not affect the obliquity distribution.

Gravitational accretion of particles onto moonlets embedded in Saturn's rings

YASUI, Yuki^{1*}; OHTSUKI, Keiji¹; DAISAKA, Hiroshi²

¹Department of Earth and Planetary Sciences, Kobe University, ²Graduate School of Commerce and Management, Hitotsubashi University

Collision and gravitational accretion of particles is an important issue related to the origin of ring-satellite systems of giant planets in the solar system. The Hill radii of Pan, Daphnis, Atlas, and Prometheus are found to be within 15 % of the observed long axes of these satellites given by the best-fit model ellipsoids. Also, the densities of these satellites ($0.4 - 0.6 \text{ g cm}^{-3}$) are very low compared to the density of water ice and all approximately equal to the critical density at that distance, which is defined as the density of a body that entirely fills its Hill sphere. From these results, the small satellites within the orbit of Pandora are thought to be formed by accretion of small porous ring particles onto large dense cores, and further accretion seems to have been suppressed when the density of the satellite reaches the critical density at that distance. Local N-body simulations also demonstrated that a Hill sphere-filling body is produced by accretion of small porous particles onto a large dense core. However, it has not been studied how the degree of particle accretion onto moonlets in the inner parts of Saturn's rings depends on the distance from Saturn.

The shapes of these small ringmoons would also provide clues to the dynamical evolution of Saturn's rings. The fact that the shapes of these ringmoons approximately match those of their associated Hill sphere suggests that the moonlet cores were surrounded by a number of particles when they were formed. On the other hand, Pan and Atlas have the characteristic shapes with equatorial ridges, and are thought to be formed by two stages. First, their precursors whose shapes are similar to their Hill sphere without equatorial ridges were formed when the rings were thick. Then, equatorial ridges were formed through particle accretion onto the equatorial planes of the above formed objects after the rings became sufficiently thin and also before ring particles diffused. However, effects of dynamical properties of the rings on the shaping of moonlets formed by particle accretion have not been examined in detail.

Propeller-shaped structures have also been found in Cassini images of Saturn's rings. These propeller-shaped features are explained by gravitational interaction between ring particles and unseen embedded moonlets. From these observations, the sizes and orbital distributions of these unseen embedded moonlets are obtained, and such information provide us with clues to the evolution of the ring-satellite system. The propeller-shaped structures are mainly observed in the A ring. Recently, observations of similar structures have also been reported for the Cassini Division, and the B and C rings. Although some of these moonlets either may be collisional shards resulting from the breakup of a bigger icy progenitor ring body or may have formed by accretion of small low-density ring particles onto larger dense fragments, the origin of these moonlets is not clear.

Using local N-body simulation, we examine gravitational accretion of ring particles onto moonlets in Saturn's rings. We find that gravitational accretion of ring particles onto moonlets is unlikely to occur at radial locations interior to the outer edge of the C ring, unless the density of the moonlets is much larger than that of water ice or non-gravitational cohesive forces play a major role. Detailed analysis of accretion process of individual particles onto moonlets shows that particle accretion onto high-latitude regions of the moonlet surface occurs even if the rings' vertical thickness is much smaller than the moonlet's radius. The degree of particle accretion in outer rings is found to depend significantly on rings' vertical thickness and optical depth. Our results suggest that large boulders recently inferred from observations of transparent holes in the C ring are likely to be collisional shards, while propeller moonlets in the A ring would be gravitational aggregates formed by particle accretion.

Keywords: gravitational accretion, moonlet, Saturn's rings

Mass-Loss Evolution of Super-Earths: Constraints on Their Compositions and Origins

KUROKAWA, Hiroyuki^{1*} ; KALTENEGGER, Lisa² ; NAKAMOTO, Taishi³

¹Nagoya University, ²Max Planck Institute for Astronomy, ³Tokyo Institute of Technology

Recent progress of the search for exoplanets, for example the transit observations with Kepler space telescope, has pushed toward small planets. Especially, "Super-Earths", that are planets having sizes from Earth to Neptune, are revealed as quite common: ~30% of solar-type stars have super-Earths (Howard et al., 2012). Therefore, an understanding of their compositions, which is related to their origins, is important for planet formation and evolution.

We can speculate the compositions of super-Earths both whose masses and radii are known by using theoretical mass-radius relations for different compositions. Some fraction of super-Earths have low density, which suggests the presence of H/He envelopes formed by protoplanetary-disk gas capture. There exist, on the other hand, high-density super-Earths possibly having rocky- or water-rich compositions. The origin of this dichotomy is one problem that we address in this study, which possibly arises from the difference of the amount of captured disk gas due to different masses and disk temperature in their formation stages, or from XUV (X-ray and EUV)-driven atmospheric escape in later evolution stages (e.g., Lopez et al., 2012). Another problem that we address in this study is "the degeneracy of composition": The compositions of super-Earths can be fitted by various ratios of H/He envelope, rock, and water. Their atmospheric compositions have been speculated by measuring their transmission spectra, but recent observations using Hubble Space Telescope suggested that cloudy atmospheres of super-Earths (Kreidberg et al., 2014; Knutson et al., 2014). If clouds are common in atmospheres of Super-Earths, direct measurements of their compositions are difficult because clouds obscure any features of atmospheric species.

In this study, we show constraints on these problems of compositions and origins of super-Earths by calculating their mass-loss evolution due to XUV-driven atmospheric escape considering the differences of host-stellar types. The ratio of XUV luminosity and bolometric luminosity differs among stellar types, which enables us to distinguish formation origin and mass-loss origin of the dichotomy of super-Earths with or without H/He envelopes. Also, the degeneracy of compositions can be solved by considering stability criteria to lose H/He envelopes.

We calculated the critical orbital radii to lose H/He envelopes for different stellar types, that corresponds to different equilibrium temperature depending on stellar types. The obtained critical separations are consistent with the distribution of the observed super-Earths with or without H/He envelopes, suggesting that the observed dichotomy has a mass-loss origin. In this case, we expect that super-Earths having moderate density and orbiting inside the critical separation are water-rich super-Earths without H/He envelope.

We also evaluated uncertainty caused by mass-loss model and XUV luminosity and discuss the validity of our results.

Keywords: exoplanet, atmospheric escape, composition, super-Earth

Exoplanet exploration for brown dwarfs with infrared astrometry

YAMAGUCHI, Masaki^{1*} ; YANO, Taihei¹ ; GOUDA, Naoteru¹

¹National Astronomical Observatory of Japan

The astrometry is one of the oldest method for the exoplanet exploration. However, only one exoplanet has been found with the method. This is because the planet mass is sufficiently smaller than the mass of the central star, so that it is hard to observe the fluctuation of the central star by the planet. Therefore, we investigate the orbital period and mass of planets which we can discover by the future astrometric satellites for brown dwarfs with the mass less than a tenth of the solar mass.

So far five planetary systems have been found, whose mass ratios are larger than a tenth. For example, for the system whose distance, orbital period and mass ratio are 10 pc, 1 year and a tenth, respectively, the apparent semi-major axis reaches 3 milli-arcsecond, which can be well detected with the future astrometric satellites such as Small-JASMINE and Gaia. With these satellite, we can discover even super-Earth for the above system.

We further investigate where in the period-mass plane we can explore the planet for individual brown dwarf with Small-JASMINE and Gaia. As a result, we find that we can explore a wide region where period and mass are within 5 years and larger than 3 earth mass. In addition, we can explore the region around 0.1 day and 10 jovian mass, where planets have never found for any central star, and where we can explore only with Small-JASMINE for most target brown dwarfs.

Keywords: astrometry, brown dwarf, exoplanet exploration, infrared, Small-JASMINE, Gaia

Experimental study on organic aerosol formation in super-Earths' atmosphere: Implications for transit observations

KOBAYASHI, Jumpei^{1*} ; SEKINE, Yasuhito² ; HONG, Peng²

¹Dept. Earth & Planet. Sci., Univ. Tokyo, ²Dept. Complexity Sci. & Engr., Univ. Tokyo

A super-Earth is an extrasolar planet with a mass greater than Earth and below Neptune. Although there is no super-Earth in our solar system, astronomical observations demonstrate that it is one of the major categories of planets beyond the solar system. Recent transit observations of super-Earths, including GJ 1214b, indicate that their atmospheres contain opaque clouds or haze at high altitudes. One candidate for the opaque materials is metallic or salt dusts, such as KCl and ZnS, which would condense in the upper atmospheres of super-Earths. Another candidate is organic haze, such as those observed in the atmosphere of Saturn's moon Titan, which would be composed of high-molecular-weight hydrocarbon aerosols produced through photochemical reactions involving CH₄. Given the proposed formation mechanisms of nearby super-Earths, e.g., planetary migration, they would have a wide variety in chemical composition of atmosphere. However, previous laboratory experiments have mainly focused on organic aerosol formation in Titan's and early Earth's atmospheres. Thus, both the formation rate and optical property of organic haze for various atmospheric compositions have been poorly constrained by laboratory experiments.

In this study, we investigate the formation rate and optical property of organic aerosols formed by laboratory experiments simulating super-Earths' atmospheres with a wide variety in chemical composition. We used initial gas mixtures of H₂ and CH₄ or CO₂ and CH₄, and varied the H₂/CH₄ or CO₂/CH₄ ratios. The experiments were conducted at a total pressure of 1 Torr in a flow system. Cold plasma irradiation was used to initiate aerosol formation. We measured the aerosol formation rate, chemical compositions of intermediate gas molecules, and optical property of aerosol using a spectroscopic ellipsometer, a quadrupole mass spectrometer, and a UV/VIS spectrometer, respectively.

Our experimental results show that the aerosol formation rate decreases with increasing the H₂/CH₄ ratio, suggesting that recycling of high-molecular-weight hydrocarbons to CH₄ occurs through reactions with H and H₂ under H₂-rich conditions. We also show that organic aerosols are produced less efficiently at higher CO₂/CH₄ ratios. The results of gas analyses also show that formation of high-molecular-weight hydrocarbons are inhibited at higher CO₂/CH₄ ratios. These results indicate that oxygen-bearing molecules and radicals formed by CO₂ dissociation oxidizes hydrocarbons produced from CH₄, which results in a lower aerosol formation rate at higher CO₂/CH₄ ratios. Optical constant of the aerosols formed under the conditions simulating super-Earths' atmospheres is significantly lower than those of Titan aerosol analogs.

Based on the experimental results, we discuss the chemical composition and formation process of transiting super-Earths, such as GJ 1214b, by comparing the observed transmittance spectra with the model spectrum. We suggest that organic aerosol production in a H₂-rich or CO₂-rich atmosphere is inefficient so that organic haze would not be capable of explaining the observed transit spectra of super-Earths, even if it contains gaseous CH₄ in the atmospheres.

Keywords: exoplanet, super-Earth, organic aerosol, haze, atmospheric composition

Transmission spectrum models of low-mass exoplanet atmospheres with haze: Application to GJ 3470b

KAWASHIMA, Yui^{1*} ; IKOMA, Masahiro¹ ; FUKUI, Akihiko² ; NARITA, Norio²

¹The University of Tokyo, ²National Astronomical Observatory of Japan

Since the first exoplanet was discovered in 1995, detection of more than 1000 exoplanets has been reported. Recently, transit observations of an exoplanet have been done at multiple wavelengths. From a decline in apparent stellar brightness due to a planetary transit, we can measure the planetary radius. In addition, observed dependence of the planetary radius on wavelength (which is often called the transmission spectrum) provides the information of absorption and scattering by molecules and small particles such as haze and clouds in the planetary atmosphere. Thus, the composition of the planetary atmosphere can be constrained by comparison between the observational and theoretical transmission spectra. The constraint on atmospheric composition gives an important clue to the origin of the planet.

Our observational group has recently observed transits of two low-mass exoplanets, GJ 3470b and GJ 1214b, at multiple wavelengths. For both planets, the observed transit radii in the optical wavelength region are greater than those in the near-infrared region, inferring the existence of haze in the atmosphere. While the observed transmission spectrum was already analysed theoretically in detail as for GJ 1214b, there are few researches discussing the theoretical spectrum models incorporating the effect of haze systematically for GJ 3470b. In this study, we have modeled theoretical transmission spectra of low-mass exoplanets orbiting close to their host stars. Then, applying the calculated spectrum models to GJ 3470b and GJ 1214b, we discuss the property of the atmospheres of both planets.

In calculating theoretical spectrum models, we have taken into account the vertical distribution of molecular abundances from the chemical equilibrium calculations, in addition to absorption and scattering of the incident radiation from the host star by molecules and haze particles in the planetary atmosphere. We explore the dependences of the atmosphere's metallicity, C/O ratio and water vapor abundances on the transmission spectrum. We also probe the dependences of haze's height, particle sizes and number density. In comparing the observed and theoretical transmission spectra, we have performed the chi-squared analysis to quantify the validity of each atmospheric model.

Keywords: exoplanets, transits, transmission spectrum models, atmospheric composition, haze

The SEEDS Exoplanet and Circumstellar Disks Survey

KUZUHARA, Masayuki^{1*}; TAMURA, Motohide²; KUDO, Tomoyuki³; HASHIMOTO, Jun⁴; KUSAKABE, Nobuhiko⁵; MATSUO, Taro⁶; MCELWAIN, Michael⁷; JANSON, Markus⁸; TAKAHASI, Yasuhiro²

¹Department of Earth and Planetary Sciences, Tokyo Institute of Technology, ²Department of Astronomy, The University of Tokyo, ³Subaru Telescope, ⁴H. L. Dodge Department of Physics and Astronomy, University of Oklahoma, ⁵National Astronomical Observatory of Japan, ⁶Department of Astronomy, Kyoto University, ⁷NASA Goddard Space Flight Center, ⁸Astrophysics Research Centre, Queen's University Belfast

About 1,000 extrasolar planets (or exoplanets) have been discovered by now. Furthermore, Kepler survey has reported the presences of more than 3,000 exoplanet candidates (Huber et al. 2013). Thus, the planetary systems are common in our Galaxy, but it has known that those exoplanets have a variety of properties. Meanwhile, studies for circumstellar disks, which are the birth-places of planets, have also progressed. In particular, the radio telescope ALMA, whose operations have recently started, have provided intriguing data for the structure properties of protoplanetary disks (e.g., van der Marel et al. 2013; Casassus 2013). ALMA should provide a deep insight to the studies of circumstellar disks.

Direct imaging observations enable the discovery and study of exoplanets orbiting their host stars at wide orbital separations comparable to a few tens of AU, but the detections of those are impractical with indirect techniques such as radial velocity or transit method. Direct imaging is also useful to characterize circumstellar disks. The high-resolution observations of scattered light from protoplanetary disks or debris-disks have provided many important clues to reveal the physical disk-planet connections. We have progressed the SEEDS project, which aims at detecting and characterizing giant exoplanets and circumstellar disks with the Subaru 8-m ground-based telescope, state-of-the-art adaptive optics AO188, and a high-sensitivity infrared camera HiCIAO that we have newly developed. The total SEEDS sample will reach 500 targets, and this target sample adequately covers stellar ages ranging from 1 to 1000 Myr for solar-type stars. Also, intermediate-mass or low-mass stars are included in our SEEDS sample. The survey is currently in its fifth year, and to date, it has identified intriguing structures, such as gaps or spirals, in more than 10 transitional or debris disks (e.g., Hashimoto et al. 2012; Grady et al. 2013). Furthermore, SEEDS has discovered a massive giant planet candidate orbiting the B-type star Kappa Andromedae (Carson et al. 2013) and a Jovian planet in orbit with a size of about 44 AU (GJ 504b) around the G0-type Sun-like star GJ 504. GJ 504b has an estimated mass of about 4 Jupiter masses and effective temperature of 500 K. Among such the wide-orbit exoplanets directly imaged so far, GJ 504b represents the lowest-mass Jovian planet, and the inferred effective temperature is the coldest. The follow-up observations for GJ 504b have revealed the presences of methane in its atmosphere (Janson et al. 2013), allowing us to report the first methane detection in an atmospheres of directly imaged exoplanet. Thus, SEEDS has successfully identified and studied the exoplanets with the previously unknown properties. After the end of SEEDS survey, the comprehensive and statistical analysis of entire survey sample will be carried out. This analysis leads to improve our understanding about exoplanets and circumstellar disks. In addition, it should become a promising clue that connects to future exoplanet/disk studies, such as a survey of extrasolar Earths.

Here, we report the latest achievements of SEEDS project, such as the detection of GJ 504b. Moreover, its whole survey status and progress are also reported, as well as the future plan of SEEDS project.

Keywords: extrasolar planet, debris disk, protoplanetary disk, giant planet, direct imaging observation